Title
Regression of murine lung tumors by the let-7 microRNA.

Journal
Oncogene, 29(11)

ISSN
0950-9232

Authors
Trang, P
Medina, PP
Wiggins, JF
et al.

Publication Date
2010-03-01

DOI
10.1038/onc.2009.445

Peer reviewed

HHS Public Access

Author manuscript

Oncogene. Author manuscript; available in PMC 2010 September 18.

Published in final edited form as:

Oncogene. 2010 March 18; 29(11): 1580–1587. doi:10.1038/onc.2009.445.

Regression of murine lung tumors by the *let-7* microRNA

Phong Trang[1,2,*], **Pedro P. Medina**[1,*], **Jason F. Wiggins**[4], **Lynnsie Ruffino**[4], **Kevin Kelnar**[4], **Michael Omotola**[4], **Robert Homer**[3], **David Brown**[4], **Andreas G. Bader**[4,5], **Joanne B. Weidhaas**[2,5], and **Frank J. Slack**[1,5]

[1] Department of Molecular, Cellular and Developmental Biology, Yale University, P.O. Box 208103, New Haven, CT 06520

[2] Department of Therapeutic Radiology, Yale University School of Medicine, P.O. Box 208040, New Haven, CT 06520

[3] Department of Pathology, Yale University School of Medicine, P.O. Box 208023, New Haven, CT 06520 and Pathology and Laboratory Medicine Service, VA Connecticut Healthcare System, 950 Campbell Ave, West Haven, CT 06516

[4] Mirna Therapeutics, Inc., a subsidiary of Asuragen Inc., 2150 Woodward St., Austin, TX 78744

Abstract

MicroRNAs (miRNAs) have recently emerged as an important new class of cellular regulators that control various cellular processes and are implicated in human diseases, including cancer. Here, we show that loss of *let-7* function enhances lung tumor formation *in vivo*, strongly supporting the hypothesis that *let-7* is a tumor suppressor. Moreover, we report that exogenous delivery of *let-7* to established tumors in mouse models of non-small cell lung cancer (NSCLC) significantly reduces tumor burden. These results demonstrate the therapeutic potential of *let-7* in NSCLC and point to miRNA replacement therapy as a promising approach in cancer treatment.

Keywords

Let-7; microRNAs; lung cancer; *K-ras*

Introduction

MicroRNAs (miRNAs) control various cellular processes such as cell death, differentiation, and development and are implicated in human diseases, including cancer (Esquela-Kerscher and Slack, 2006). Aberrant expression of specific miRNAs is associated with tumorigenesis

[5]Corresponding authors: Dr FJ Slack, Department of Molecular, Cellular and Developmental Biology, KBT 936, Yale University, PO Box 208103, 266 Whitney Avenue, New Haven, CT 06520, USA. frank.slack@yale.edu or Dr J Weidhaas, Department of Therapeutic Radiology, Yale University School of Medicine, PO Box 208040, New Haven, CT 06520, USA. joanne.weidhaas@yale.edu.
*These authors contributed equally to this work

Conflict of interest

FS and JW are inventors on pending patent applications in the miRNA area. Part of this work was supported by a grant to FS from Asuragen.

and miRNA coding genes are often found in fragile genomic regions gained and lost in cancers (Calin *et al.*, 2004b; Sevignani *et al.*, 2007). Many members of one miRNA family in particular, *let-7*, map to chromosomal regions frequently deleted in lung cancer (Calin *et al.*, 2004b), and reduced *let-7* expression in non-small cell lung cancer (NSCLC) patients is correlated with poor prognosis (Takamizawa *et al.*, 2004; Yanaihara *et al.*, 2006). Moreover, *let-7* miRNAs are thought to function as tumor suppressors through their negative regulation of multiple oncogenes, such as *RAS*, *MYC*, *HMGA2*, and promoters of cell cycle progression, such as *CDC25A*, *CDK6*, and Cyclin D2 (Johnson *et al.*, 2007; Johnson *et al.*, 2005; Lee and Dutta, 2007; Mayr *et al.*, 2007; Park *et al.*, 2007; Sampson *et al.*, 2007; Yu *et al.*, 2007). Administration of *let-7* blocks the growth of cultured lung cancer cells and also prevents the onset of tumor formation in a mouse model of NSCLC (Esquela-Kerscher *et al.*, 2008; Johnson *et al.*, 2007; Kumar *et al.*, 2008).

Materials and Methods

Lung cancer xenografts

Human H460 non-small cell lung carcinoma cells were cultured in RPMI media (Invitrogen, Carlsbad, CA) following standard tissue culture procedures. H460 cells were trypsinized, counted and subcutaneously injected into the lower back of 6–8 week old NOD/SCID mice (Jackson Laboratories, Bar Harbor, MA) using 3×10^6 cells in 100 μl RPMI with 50% matrigel (BD Biosciences, San Jose, CA) per injection. Once cancer cells have developed palpable tumors caliper measurements were taken daily and tumor volume was calculated using the formula $V = \text{length} \times \text{width}^2/2$, in which the length is greater than the width. When tumors reached an average volume of 150 mm^3, 50 μl synthetic miRNA complexed with the siPORTamine transfection reagent (Ambion) was delivered intratumorally in 3-day intervals. Synthetic miRNAs are double-stranded and ready-to-use miRNA mimics and were purchased from Ambion, Life Technologies, Austin, TX (pre-miR; cat. no. AM17100). For each injection, 6.25 ug miRNA was complexed with 1.6 μl siPORTamine (Ambion; cat. no. AM4502) reagent in 50 μl phosphate-buffered saline. Mice were sacrificed by CO_2 inhalation either one or three days after the last treatment, and tumors were collected and prepared for histology and RNA isolation. All animal experiments were performed under an IACUC approved animal study protocol.

Quantitative real-time PCR

Total RNA from H460 tumors was isolated using the mirVANA PARIS RNA isolation kit (Ambion, Austin, TX) following manufacturer's instructions. For RT-PCR detection of *let-7* mRNA targets in H460 xenografts, 500 ng purified RNA was reverse transcribed with random decamers using MMLV-RT (cat. no. 28025-021, Invitrogen, Carlsbad, CA) with the following incubations: 42°C for 60 min; 85°C for 5 min. For RT-PCR detection of the *let-7b* oligonucleotide, 10 ng purified RNA was heat-denatured at 70 °C for 2 min and reverse transcribed using the *let-7b* TaqMan miRNA Assay (Applied Biosystems, Foster City, CA) with the following conditions: 16°C for 30 min; 42°C for 30 min; 85°C for 5 min and MMLV-RT (Invitrogen). Gene and *let-7b* expression levels were determined by real-time PCR using Platinum Taq Polymerase reagents (Invitrogen) on the ABI Prism 7900 SDS (Applied Biosystems). TaqMan Gene Expression Assays (Applied Biosystems) were used

with the following cycling conditions: 95°C for 1 min (initial denature); then 50 cycles of 95°C for 5 sec, 60°C for 30 sec. The 18S rRNA was amplified as an internal reference to adjust for well-to-well variances in amount of starting template. The *let-7b* TaqMan miRNA Assay (Applied Biosystems) was used with the following cycling conditions: 95°C for 1 min (initial denature); then 50 cycles of 95°C for 15 sec, 60°C for 1 min. Total copy numbers of *let-7b* molecules in tumor tissues were calculated using a standard curve generated with 10^3–10^{12} *let-7b* copies amplified on the same plate. Quantification of levels of *let-7a*, was performed using the Taqman microRNA PCR system (ABI, per standard protocol). Levels were normalized to mice treated with Ad-*Cre* alone (baseline) to determine changes in expression levels 4 weeks post lentivirus infection.

Tumor histologies and immunohistochemistries

Tumor tissues were fixed in formalin and embedded in paraffin using the Microm Tissue Embedding Center (Labequip, Ltd.; Markham, Ontario, Canada). 5 μm tissue sections were prepared and stained with hematoxylin and eosin (H&E) according to standard protocols. For immunohistochemistries, primary antibodies specific for Ki-67 (cat. no. M7249; DAKO, Carpinteria, CA), active Caspase-3 (cat. no. AF835; R&D Systems, Minneapolis, MN), N-Ras (cat. no. sc-20; Santa Cruz Biotechnology, Santa Cruz, CA) and CDC25A (cat. no. sc-97; Santa Cruz Biotechnology) were used. All antibodies were visualized by secondary horseradish peroxidase-conjugated immunoglobulins (cat. no. ab6721; Abcam, Cambridge, MA). Briefly, slides were washed in tris-buffered saline (TBS; 10 mM Tris, 150 mM NaCl, pH 7.6) and incubated in 3% (v/v) hydrogen peroxide for 10 min to suppress endogenous activity. Slides were washed with TBS and incubated in 5% (v/v) normal goat serum (cat. no. 005-000-001; Jackson ImmuResearch Laboratories, Inc., West Grove, PA) diluted in incubation buffer (0.1% [w/v] BSA in TBS) to reduce nonspecific binding of antibodies. Slides were incubated with primary antibodies in incubation buffer overnight at 4°C. After several washes in TBS, secondary antibodies were added and incubated for 60 min at room temperature. Secondary antibodies were visualized by adding 3,3′-diaminobenzidine (DAB; cat. no. K3465; DAKO) for 2–5 minutes, followed by several washing steps. Negative controls were performed by omitting the primary antibody. The slides were counterstained with hematoxylin for 10 seconds and mounted on cover slips with mounting medium (cat. no. 4112; Richard-Allan Scientific, Kalamazoo, MI). For determining apoptotic bodies by TUNEL assay, ApopTag Plus Peroxidase In Situ Apoptosis Kit (Chemicon, Temecula, CA, USA) was used according to the manufacturer's instructions.

Anti-scr and anti-let-7 synthesis

The anti-miRs were synthesized by the Keck Facility (Yale University New Haven, CT, USA). To enhance their stability the anti-miRs were generated using 2′-O-methyl-modified nucleotides (italic) and phosphorothioate bonds (*) as follows:

anti-*let-7g*: 5′ ***A*C*UGUACAAACUACUACCU*C*A*** 3′;

anti-*scramble*: 5′***C*U*CAACAACGUAUAUUCAG*C*A*** 3′.

The anti-*scramble* RNA was designed using the *Scramble RNA* software to have same GC% than *anti-let-7g* but no homology with the mouse genome (Levenkova *et al.*, 2004). The anti-miR-reporter has a fluorescein amidite (FAM) attached at 5′ of anti-*let-7g* to follow their delivery using a fluorescent microscope with GFP detection wavelengths.

In vivo adenoviral infection and anti-miR delivery to LSL-K-ras G12D mice

Approximately 6-week-old *LSL-K-ras G12D* animals were anesthetized with an isoflurane/propylene glycol mixture and intranasally co-inoculated with adenovirus and anti-miRs (anti-*let-7g* or scrambled). The protocol was adapted from (Bitko and Barik, 2008; Bitko *et al.*, 2005; Esquela-Kerscher *et al.*, 2008; Jackson *et al.*, 2001): 5×10^8 PFU of Ad-*Cre*, 60 μg of anti-miR and 0.01M $CaCl_2$ were mixed in a final volume of 125 μl of MEM and inoculated to the mice in two 62.5 μL instillations as described (Jackson *et al.*, 2001). Ad-*Cre*, used to induce tumor formation in *LSL-K-ras G12D* mice, was purchased from the Gene Transfer Vector Core Facility at the University of Iowa. Mice were sacrificed 7 weeks post-infection, and the PBS-perfused lungs were retained for analysis. Lungs were prepared for histological analysis to examine tumor burden by fixing the tissue in 4% paraformaldehyde overnight, embedded in paraffin and stained with hematoxylin and eosin. The delivery of anti-miRs in the lung was tested using anti-miR-5′ FAM oligonucleotides using a fluorescent microscope. Ad-*Cre* recombination was tested using a PCR assay to verify that *K-ras G12D* mice had undergone *Cre*-mediated removal of the stop element at the mutant *K-ras* locus as previously described (Jackson *et al.*, 2001). Lung and tumor areas were quantified using ImageJ software in manual measurement mode as described previously (Esquela-Kerscher *et al.*, 2008). The overall tumor burden was measured as a ratio of total tumor area to total lung area by taking the average of every seventh slide section throughout the lung. Nomenclature based on that of Nikitin et al.(Nikitin *et al.*, 2004).

Viral constructs and in vivo infection

Adenovirus expressing *Cre*-recombinase was obtained as described previously (Jackson *et al.*, 2001). Lentivirus expressing *let-7a* was purchased from Select Biosciences (Mountain View, CA). *LSL-K-ras G12D* (Jackson *et al.*, 2001) (strain number 01XJ6) mice were obtained from the NCI-Frederick Mouse Repository and treated with Adenovirus and Lentivirus as described previously (Esquela-Kerscher *et al.*, 2008).

Results

In vivo anti-*let-7* delivery to lungs leads to increased tumor burden

Available data suggest that the *let-7* miRNA functions as a tumor suppressor that is frequently lost in non-small cell lung cancer (NSCLC) (Johnson *et al.*, 2005; Takamizawa *et al.*, 2004; Yanaihara *et al.*, 2006), yet no loss of function assays have been reported to formally test this hypothesis. The mouse *let-7* miRNA family consists of multiple members, encoded by 12 genes in the mouse genome, nine of which code for unique mature *let-7* molecules, and three that code for redundant sequences (Roush and Slack, 2008). We previously showed that five of the *let-7* family members, *let-7a*, *let-7b*, *let-7c*, *let-7d*, and *let-7g* consistently reduced the number of proliferating A549 and HepG2 cells by similar

levels (Johnson *et al.*, 2007). Because we have not yet detected a difference with any particular *let-7* family member, this suggests functional redundancy. Since it is likely that their biological functions overlap, *in vivo* loss of functional genetic tests with the *let-7* family are technically difficult. To circumvent this difficulty, we developed a novel protocol to test the role of *let-7* family members as tumor suppressors in a well-characterized *K-ras* autochthonous NSCLC mouse model lung (Jackson *et al.*, 2001), *LSL-K-ras G12D,* containing a Cre recombinase dependent allele of activated *Kras* with endogenous 5′ and 3′ regions. We combined a successful protocol for delivery of small RNAs by intranasal passage (Bitko and Barik, 2008; Bitko *et al.*, 2005) with established *in vivo* antisense technology (Krutzfeldt *et al.*, 2005). We designed an anti-miR molecule targeting the *let-7g* sequence (anti-*let-7g*) and a control with same GC percentage but no homology in the mouse genome (anti-*scrambled (scr)*) (See Materials and Methods for details). We chose *let-7g* for this experiment because *let-7g* maps to 3p21 which has been implicated in the initiation of human lung cancers (Calin *et al.*, 2004a) and also because there is evidence suggesting that *let-7g* mediated tumor suppression is especially potent in tumors harboring oncogenic *K-ras* mutations (Kumar *et al.*, 2008). However, we did not rule out the possibility that our anti-*let-7g* molecule cross-reacts with other *let-7* family members due to their high similarity.

To monitor the delivery of anti-miRs to the lung, we labeled the anti-miR with a FAM molecule attached at its 5′OH. We inoculated this labeled anti-miR into mouse lungs by intranasal passage and harvested their lungs 2 hours (h) and 16h later. Both time points showed similar fluorescence signal in the lung (Suppl Fig. 1), demonstrating efficient and quick up-take of the modified RNAs. These observations match previously reported data from Bitko et al.(Bitko and Barik, 2008) showing that naked siRNAs can be successfully delivered to the lung via intranasal passage and remain stable.

We transiently delivered non-labeled anti-miRs to mice carrying a knock-in activated *K-rasG12D* allele, that we had simultaneously inoculated with an adenovirus expressing *Cre* recombinase (Ad-*Cre*) to activate *LSL-K-ras G12D* (Suppl. Fig 2) and initiate lung tumors (as described in Esquela-Kerscher et al. (Esquela-Kerscher *et al.*, 2008)). In both cases, the lungs show a range of proliferative lesions including bronchiolar papillary hyperplasia, adenoma, atypical adenomatous hyperplasia and focal low grade adenocarcinoma. However, mice treated with anti-*let-7g* (n=5) displayed more extensive ($p<0.01$) tumor burden 7 weeks after intranasal inoculation relative to anti-*scr* control (n=5) with more prominent bronchiolar papillary hyperplasia (Fig. 1). We speculate that transient knock-down of *let-7g* (and potentially other *let-7* family members) function enhances tumorgenicity by elevating levels of *let-7* target genes soon after delivery. This could act synergistically with the *K-ras* mutation to form a more aggressive NSCLC phenotype similar to the case of the double mutant mouse model *K-ras* G12D; Trp-$53^{flox/flox}$ (Jackson *et al.*, 2005). This experiment demonstrates a role for *let-7* in the suppression of lung tumors via *K-ras* (Johnson *et al.*, 2005) *in vivo* and is strong evidence that *let-7* functions as a tumor suppressor in the lung.

Intratumoral delivery of *let-7* reduces tumor size in a lung cancer xenograft model

To study the anti-tumorigenic role of *let-7* in lung cancer, we had previously examined two murine models of human lung cancer, a xenograft model using human lung cancer cells and the *LSL-K-ras*-G12D model. In the latter mouse model, tumorigenesis was initiated by the activation of a gain of function *K-ras G12D* gene through the inhalation of Ad-*Cre* (Jackson *et al.*, 2001) as described above. Using these models, we showed that *let-7* suppresses lung tumor initiation, resulting in a 66% reduction of tumor burden when comparing *K-ras G12D* mice treated with *let-7* miRNA to those that were treated with a control miRNA, respectively (Esquela-Kerscher *et al.*, 2008). Similar findings were made by the Jack's lab (Kumar *et al.*, 2008). Since in both studies the *let-7* miRNA was delivered at the same time as tumorigenesis was initiated, these two studies showed that *let-7* may be useful as a preventive therapy against lung cancer in the *LSL-K-ras G12D* mice. While these results revealed an inherent anti-oncogenic activity of *let-7* during tumorigenesis, the therapeutic potential of *let-7* on established tumors remained unknown.

Because most newly diagnosed cases of NSCLC are locally advanced or metastatic at presentation and refractory to most currently applied therapies (Isobe *et al.*, 2005), we explored the therapeutic potential of *let-7* in established tumors. Immunodeficient NOD/SCID mice were subcutaneously inoculated with human H460 lung cancer cells and housed until the tumor cells – initially loosely distributed in matrigel – had formed solid and palpable tumors with an average volume of 100–150 mm^3. We chose the H460 cell line for this study because it is among the most aggressively growing NSCLC xenografts and is among the cell lines most resistant to other targeted therapies (Hohla *et al.*, 2007; Siegfried *et al.*, 1999). Beginning on day 11 following inoculation, *let-7b* or a negative control miRNA (miR-NC) were repeatedly administered by intratumoral injections every 3 days. These synthetic miRNAs were complexed with siPORTamine (siPORT), a lipid-based transfection reagent that enhances cellular uptake of the oligonucleotide. All mice were sacrificed once control animals developed tumors that exceeded an average volume of 600 mm^3 (day 21). As shown in Figure 2A, mice that received miR-NC developed tumors at a pace similar to those treated with siPORT alone or phosphate-buffered saline (PBS). In contrast, local delivery of synthetic *let-7b* induced a specific inhibitory response and robustly interfered with tumor growth. Images of tumor-bearing mice on the day of sacrifice are shown in Figure 2B.

A histological analysis revealed that tumors treated with miR-NC or siPORT were densely packed with viable H460 cells and only occasionally contained small necrotic areas (Fig. 2C, left panel, center and bottom). These pockets of dead cells are likely due to the aggressive nature of H460 cells that rapidly outgrow other cancer cells and compete for blood supply and nutrients (Edinger and Thompson, 2004). Tumors that received *let-7b*, however, contained large areas filled with cell debris (Fig. 2C, left panel, top). These tumors also had enlarged necrotic cores in agreement with the supposition that intratumoral injections preferentially deliver the therapeutic to the center of the tumor. To get better insight into the mechanism of action, we performed immunohistochemistry stains using antibodies specific for the Ki-67 and caspase 3 proteins, markers for cellular proliferation and apoptosis, respectively. As shown in Figure 2C (right panel), H460 cells displayed

reduced levels of Ki-67 in response to *let-7b* treatment. In contrast, caspase 3 levels remained unaltered. It is possible that *let-7* does not specifically induce the apoptotic cascade or alternatively, apoptosis induced by *let-7* occurred immediately after administration and is no longer detectable at the time of the analysis. This observation is in accord with our previous observations and indicates a role for *let-7* over-expression in interfering with cell cycle progression rather than a major role in directly inducing programmed cell death (Esquela-Kerscher *et al.*, 2008; Johnson *et al.*, 2007).

To better correlate the therapeutic response with the delivery of *let-7b*, we determined the presence of *let-7b* oligonucleotides in tumor tissues 24 hours after the final administration. Total RNA from H460 tumors treated with *let-7b*, miR-NC, siPORT or PBS were analyzed by quantitative real-time PCR (qRT-PCR) using *let-7b* specific primers. Tumors injected with the *let-7b* oligo contained ~14-fold more *let-7b* miRNA compared to the endogenous levels that are present in the controls (Fig. 3A). Since crude tumor tissue was used for this analysis, these levels include extracellular as well as intracellular *let-7b*. To confirm that the synthetic *let-7b* has successfully been delivered into the cytoplasm of H460 tumor cells and actively engages in the RNA-induced silencing pathway, we evaluated the mRNA levels of *NRAS* and *CDK6*, both of which are directly targeted by the *let-7* miRNA(Esquela-Kerscher *et al.*, 2005; Johnson *et al.*, 2007). We chose *N-ras* as a readout for *let-7* activity because unlike the *K-ras* mRNA, *N-ras* mRNA seems to undergo degradation in response to *let-7* treatment (Johnson *et al.*, 2005). As shown in Figure 3B, both transcripts were strongly repressed in tumors that have been injected with the *let-7b* miRNA. Hence, these mRNA levels inversely correlate with increased accumulation of *let-7b* in these tumors, illustrating the successful cellular uptake of the synthetic *let-7* mimetic (see Fig. 3A). In addition, the down-regulation of *let-7* targets was confirmed on the protein level by immunohistochemistry directed against proteins for which suitable antibodies were available (Fig. 3C). Similar to the reduction of the mRNA, tumors treated with *let-7b* lacked expression of NRAS protein relative to tumors that received either miR-NC or siPORT. CDC25A protein, another *let-7* target that was less responsive on the mRNA level, also showed reduced protein expression in tumors that were injected with *let-7b* (Johnson *et al.*, 2007). Thus, the synthetic *let-7b* miRNA successfully entered H460 tumor cells and activated the *let-7* silencing pathway to suppress its targets and reduce tumor growth.

Intranasal delivery of *let-7* reduces established K-ras dependent lung tumors

To address whether *let-7* miRNA can reduce tumor burden in late stage *K-ras G12D* animal lungs, 5×10^8 plaque-forming units (p.f.u) of Ad-*Cre* were administered intranasally to six-week-old *LSL-Kras-G12D* mice and the mice were maintained for 10 weeks. The 10 weeks post-infection group was split into 3 sets. One set acted as a baseline for the study (n=6) (Fig. 4A, bottom, left and center panels,). A second set was treated with 1×10^6 infectious units (i.f.u) of a lentiviral vector expressing *let-7a* (lenti-*let-7* that showed a three to four fold up-regulation of *let-7* miRNA in A549 cells (Suppl Fig. 3)). The third set was treated with a control empty lentiviral vector (lenti-control). Baseline animals were sacrificed at 10 weeks post Ad-Cre infection. All other animals were incubated further and sacrificed either 2 or 4 weeks post lentivirus infection, and lung morphology, cell proliferation and apoptosis were assessed immunohistochemically. We observed similar lung morphology for both

baseline mice and lenti-control mice that were sacrificed at 2 and 4 weeks post lentivirus infection. Baseline mice and lenti-controls showed bronchiolar papillary hyperplasia and extensive replacement of the parenchyma predominantly by papillary adenocarcinoma (Figure 4A lower two rows, Fig 4B, suppl Fig 4). In mice given lenti-*let-7*, we observed residual bronchiolar papillary hyperplasia but markedly reduced parenchymal tumor burden when compared to those treated with the lenti-control (75% reduction in tumor area) and the baseline animals (64% reduction), respectively (Fig. 4A, Top; Fig. 4B; Suppl Fig. 4). Also, a qRT-PCR analysis revealed that lungs from mice treated with lenti-*let-7* contained ~5-fold more *let-7* oligonucleotides compared to controls (Suppl. fig. 5A). These results show that *let-7* can effectively cause remission of lung tumors in an advanced *K-ras* activated NSCLC mouse model.

To evaluate the form of cell death *in vivo*, we performed TdT-mediated dUTP nick end labeling (TUNEL) assays and Ki67 staining to measure the level of apoptosis and proliferation, respectively. Consistent with the H460 xenograft model, *let-7* treated lungs, the control and baseline lungs showed similar levels of TUNEL-positive cells (Suppl fig. 4B). In contrast, *let-7* treated lungs lacked Ki67, suggesting that *let-7* over-expression interfered with proliferation of tumor cells in lungs with activated *K-ras* G12D (Fig. 4A, top, right panel). Therefore, we conclude that *let-7* blocks tumor growth by repressing proliferation and eliminating tumor cells potentially through a non-apoptotic mechanism. Apoptosis-unrelated cell death as a means to eliminate cancer cells is a common mechanism of many therapeutic agents and is reminiscent of the prevailing form of cell death in solid tumors after cytotoxic therapy (Brown and Wilson, 2003). *Let-7* over-expression may lead to cytotoxic-type damage or may disrupt DNA repair pathways that would correct for naturally occurring damage in the quickly dividing cancer cells.

Discussion

While much work remains to be done to determine the tumor-suppressive mechanism of *let-7* in *in vivo* lung tumors, studies from our lab, the Jack's group, and others suggest that *let-7* may act through direct repression of the *Kras*, *HMGA2*, and *c-Myc* oncogenes (Johnson *et al.*, 2005; Kumar *et al.*, 2008; Lee and Dutta, 2007; Sampson *et al.*, 2007). Although *Kras* might seem to be a critical target in this mouse model, we speculate that other targets are also important, as a recent study showed that the sole inhibition of c-Myc resulted in significant inhibition of tumor formation in early stage, and reduction of tumors in late stage *K-ras* activated lungs (Soucek *et al.*, 2008).

In conclusion, our studies show that *let-7* is a tumor suppressor in lung cancer, and provide proof-of-concept for *let-7* replacement therapy as a novel and promising modality to treat lung cancer. Similar to targeted therapies that tackle a gain-of-function in cancer, such as EGFR inhibitors, the reintroduction of the *let-7* tumor suppressor miRNA interferes with the oncogenic properties of tumor cells and induces a therapeutic response. In contrast to an inhibitory approach, however, "miRNA replacement therapy" seeks to restore expression and function of a naturally occurring molecule. Hence, miRNA replacement therapy represents a unique therapeutic opportunity following a different strategy than small molecule inhibitors, siRNAs and miRNA antagonists, and deserves further exploration. This

approach has been successfully demonstrated for liver and metastatic prostate cancer (Kota *et al.*, 2009; Takeshita *et al.*, 2009). While our results presented here suggest that *let-7* miRNAs may prove useful in the treatment of human NSCLC, the challenge of a *let-7* therapy will be the successful delivery of the miRNA to the tumor cells. Local delivery of synthetic *let-7* by intratumoral injections resulted in strong inhibition of overall tumor growth. However, this delivery route might be inadequate in a clinical setting as peripheral tumor cells remained present and showed limited knock-down of *let-7* targets by immunohistochemistry. Therefore, a delivery technology that facilitates universal access to all tumor cells, such as a systemic delivery route, might be needed to make a *let-7* therapeutic more efficacious. Alternatively, adenoviral or retroviral delivery of *let-7*, as demonstrated here, could become useful tools in the treatment of respiratory malignancies.

Supplementary Material

Refer to Web version on PubMed Central for supplementary material.

Acknowledgments

We would like to acknowledge Xianping Liang for help with animal husbandry and genotyping, and Paul Lebourgeois for histopathological analyses. PT was supported by a NIH NRSA postdoctoral fellowship (F32CA130376). PM was supported by a postdoctoral fellowship from Ministry of Education and Science of Spain (MEC) and from the Hope Funds for Cancer Research. JBW was supported by the ASTRO Junior Faculty Career Research Training Award. FJS and JBW were supported by grants from the NIH (CA131301-01A1) and from the Connecticut Department of Public Health (RFP #2006-0913).

References

Bitko V, Barik S. Nasal delivery of siRNA. Methods Mol Biol. 2008; 442:75–82. [PubMed: 18369779]

Bitko V, Musiyenko A, Shulyayeva O, Barik S. Inhibition of respiratory viruses by nasally administered siRNA. Nat Med. 2005; 11:50–5. [PubMed: 15619632]

Brown JM, Wilson G. Apoptosis genes and resistance to cancer therapy: what does the experimental and clinical data tell us? Cancer Biol Ther. 2003; 2:477–90. [PubMed: 14614312]

Calin GA, Liu C-G, Sevignani C, Ferracin M, Felli N, Dumitru CD, et al. MicroRNA profiling reveals distinct signatures in B cell chronic lymphocytic leukemias. Proceedings of the National Academy of Sciences. 2004a; 101:11755–11760.

Calin GA, Sevignani C, Dumitru CD, Hyslop T, Noch E, Yendamuri S, et al. Human microRNA genes are frequently located at fragile sites and genomic regions involved in cancers. Proc Natl Acad Sci U S A. 2004b; 101:2999–3004. [PubMed: 14973191]

Edinger AL, Thompson CB. Death by design: apoptosis, necrosis and autophagy. Curr Opin Cell Biol. 2004; 16:663–9. [PubMed: 15530778]

Esquela-Kerscher A, Johnson SM, Bai L, Saito K, Partridge J, Reinert KL, et al. Post-embryonic expression of C. elegans microRNAs belonging to the lin-4 and let-7 families in the hypodermis and the reproductive system. Dev Dyn. 2005; 234:868–77. [PubMed: 16217741]

Esquela-Kerscher A, Slack FJ. Oncomirs - microRNAs with a role in cancer. Nat Rev Cancer. 2006; 6:259–69. [PubMed: 16557279]

Esquela-Kerscher A, Trang P, Wiggins JF, Patrawala L, Cheng A, Ford L, et al. The let-7 microRNA reduces tumor growth in mouse models of lung cancer. Cell Cycle. 2008; 7:759–64. [PubMed: 18344688]

Hohla F, Schally AV, Kanashiro CA, Buchholz S, Baker B, Kannadka C, et al. Growth inhibition of non-small-cell lung carcinoma by BN/GRP antagonist is linked with suppression of K-Ras, COX-2, and pAkt. Proc Natl Acad Sci U S A. 2007; 104:18671–6. [PubMed: 18003891]

Isobe T, Herbst RS, Onn A. Current management of advanced non-small cell lung cancer: targeted therapy. Semin Oncol. 2005; 32:315–28. [PubMed: 15988686]

Jackson EL, Olive KP, Tuveson DA, Bronson R, Crowley D, Brown M, et al. The differential effects of mutant p53 alleles on advanced murine lung cancer. Cancer Res. 2005; 65:10280–8. [PubMed: 16288016]

Jackson EL, Willis N, Mercer K, Bronson RT, Crowley D, Montoya R, et al. Analysis of lung tumor initiation and progression using conditional expression of oncogenic K-ras. Genes Dev. 2001; 15:3243–8. [PubMed: 11751630]

Johnson CD, Esquela-Kerscher A, Stefani G, Byrom M, Kelnar K, Ovcharenko D, et al. The let-7 microRNA represses cell proliferation pathways in human cells. Cancer Res. 2007; 67:7713–22. [PubMed: 17699775]

Johnson SM, Grosshans H, Shingara J, Byrom M, Jarvis R, Cheng A, et al. RAS is regulated by the let-7 microRNA family. Cell. 2005; 120:635–47. [PubMed: 15766527]

Kota J, Chivukula RR, O'Donnell KA, Wentzel EA, Montgomery CL, Hwang HW, et al. Therapeutic microRNA delivery suppresses tumorigenesis in a murine liver cancer model. Cell. 2009; 137:1005–17. [PubMed: 19524505]

Krutzfeldt J, Rajewsky N, Braich R, Rajeev KG, Tuschl T, Manoharan M, et al. Silencing of microRNAs in vivo with 'antagomirs'. Nature. 2005; 438:685–9. [PubMed: 16258535]

Kumar MS, Erkeland SJ, Pester RE, Chen CY, Ebert MS, Sharp PA, et al. Suppression of non-small cell lung tumor development by the let-7 microRNA family. Proc Natl Acad Sci U S A. 2008; 105:3903–8. [PubMed: 18308936]

Lee YS, Dutta A. The tumor suppressor microRNA let-7 represses the HMGA2 oncogene. Genes Dev. 2007; 21:1025–30. [PubMed: 17437991]

Levenkova N, Gu Q, Rux JJ. Gene specific siRNA selector. Bioinformatics. 2004; 20:430–2. [PubMed: 14960474]

Mayr C, Hemann MT, Bartel DP. Disrupting the pairing between let-7 and Hmga2 enhances oncogenic transformation. Science. 2007; 315:1576–9. [PubMed: 17322030]

Nikitin AY, Alcaraz A, Anver MR, Bronson RT, Cardiff RD, Dixon D, et al. Classification of proliferative pulmonary lesions of the mouse: recommendations of the mouse models of human cancers consortium. Cancer Res. 2004; 64:2307–16. [PubMed: 15059877]

Park SM, Shell S, Radjabi AR, Schickel R, Feig C, Boyerinas B, et al. Let-7 prevents early cancer progression by suppressing expression of the embryonic gene HMGA2. Cell Cycle. 2007; 6:2585–90. [PubMed: 17957144]

Roush S, Slack FJ. The let-7 family of microRNAs. Trends Cell Biol. 2008; 18:505–16. [PubMed: 18774294]

Sampson VB, Rong NH, Han J, Yang Q, Aris V, Soteropoulos P, et al. MicroRNA let-7a down-regulates MYC and reverts MYC-induced growth in Burkitt lymphoma cells. Cancer Res. 2007; 67:9762–70. [PubMed: 17942906]

Sevignani C, Calin GA, Nnadi SC, Shimizu M, Davuluri RV, Hyslop T, et al. MicroRNA genes are frequently located near mouse cancer susceptibility loci. Proc Natl Acad Sci U S A. 2007; 104:8017–22. [PubMed: 17470785]

Siegfried JM, Krishnamachary N, Gaither Davis A, Gubish C, Hunt JD, Shriver SP. Evidence for autocrine actions of neuromedin B and gastrin-releasing peptide in non-small cell lung cancer. Pulm Pharmacol Ther. 1999; 12:291–302. [PubMed: 10545285]

Soucek L, Whitfield J, Martins CP, Finch AJ, Murphy DJ, Sodir NM, et al. Modelling Myc inhibition as a cancer therapy. Nature. 2008; 455:679–83. [PubMed: 18716624]

Takamizawa J, Konishi H, Yanagisawa K, Tomida S, Osada H, Endoh H, et al. Reduced expression of the let-7 microRNAs in human lung cancers in association with shortened postoperative survival. Cancer Res. 2004; 64:3753–6. [PubMed: 15172979]

Takeshita F, Patrawala L, Osaki M, Takahashi RU, Yamamoto Y, Kosaka N, et al. Systemic Delivery of Synthetic MicroRNA-16 Inhibits the Growth of Metastatic Prostate Tumors via Downregulation of Multiple Cell-cycle Genes. Mol Ther. 2009

Yanaihara N, Caplen N, Bowman E, Seike M, Kumamoto K, Yi M, et al. Unique microRNA molecular profiles in lung cancer diagnosis and prognosis. Cancer Cell. 2006; 9:189–98. [PubMed: 16530703]

Yu F, Yao H, Zhu P, Zhang X, Pan Q, Gong C, et al. let-7 regulates self renewal and tumorigenicity of breast cancer cells. Cell. 2007; 131:1109–23. [PubMed: 18083101]

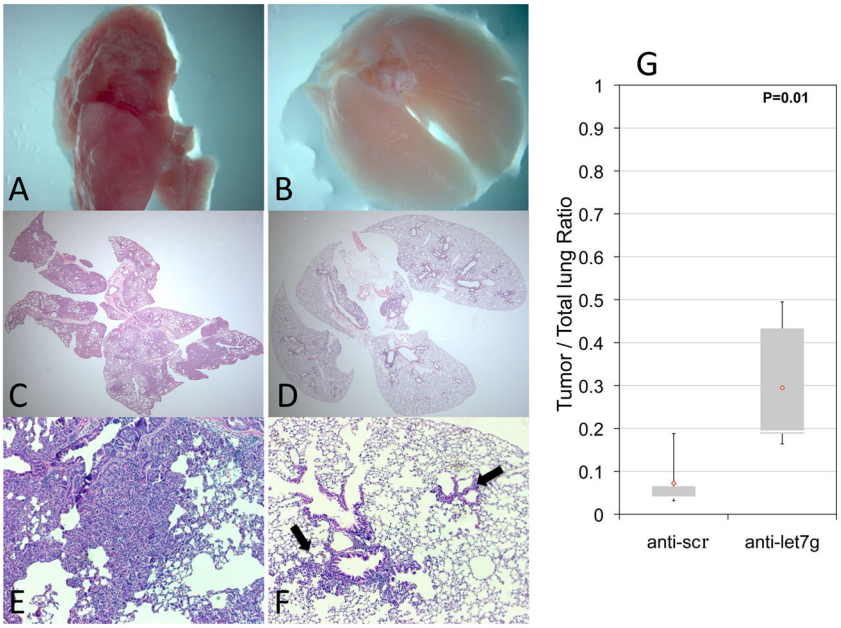

Figure 1. Anti-*let-7* enhances tumor formation in activated *K-ras* lungs

Macroscopic observation of the *K-ras G12D* mice lungs seven weeks after infection with Ad-*Cre*. The lung surface of the mice treated with anti-*let-7* (A, C) shows higher levels of precancerous lesions in comparison with the lungs treated with anti-*scr* (B, D). This observation correlates with a higher load of neoplastic development observed histologically (C, D). Slides stained by H&E x100 amplified show advanced tumor development in lungs treated with anti-*let-7* ((E) extended adenoma with acinar and papillar structures) in comparison with the lungs treated with anti-*scr* ((F) earlier neoplastic lesions such as adenomatous and epithelial hyperplasia shown with arrow). G. Quantification of total tumor area. The ratios of tumor area versus normal lung area are presented as a box-and-whisker plot. Boxes represent interquartile ranges (between the 25^{th} and 75^{th} quartiles) and the two-tailed p-value is indicated. The total range, mean (◇), and median (blank bar) are shown.

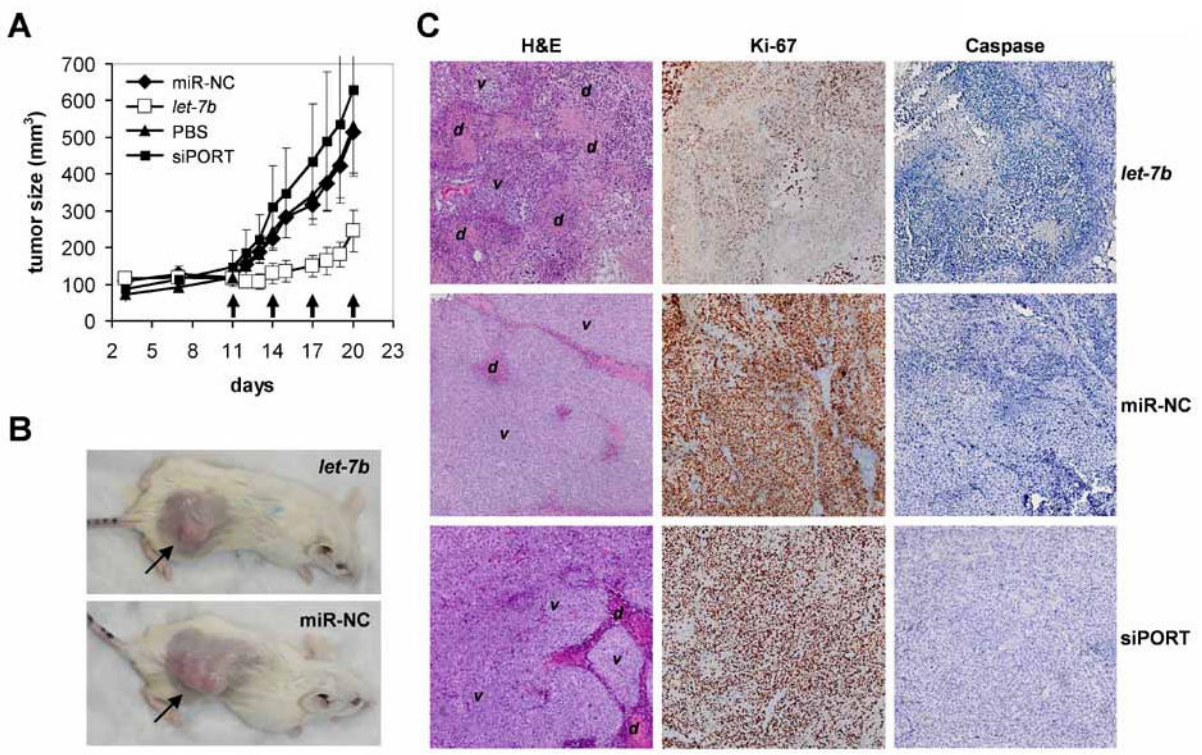

Figure 2. Growth inhibition of established lung tumor xenografts by synthetic *let-7* oligonucleotides

(**A**) Three × 10^6 H460 lung cancer cells in 50% matrigel were subcutaneously injected into immunodeficient NOD/SCID mice. On days 11, 14, 17 and 20, synthetic *let-7b* or miR-NC double-stranded and ready-to-use miRNAs conjugated with the siPORTamine transfection reagent were intratumorally delivered into groups of six animals. As additional negative controls, tumor-bearing mice received intratumoral injections of PBS (n=5) or the lipid formulation lacking any oligonucleotide (siPORT; n=6). Caliper measurements were taken to determine the length and width of each tumor and to calculate total tumor volumes. Standard deviations are shown in the graph. Arrows indicate days of treatment. (**B**) Images of mice carrying H460 tumors after sacrifice on day 21. Subcutaneous lung tumors are indicated by arrows. **(C)** Tumor histologies and immunohistochemistry staining specific for Ki-67 and active caspase 3 are shown. *v*, area containing viable H460 tumor cells; *d*, area containing dead cells, cell debris or cells undergoing cell death. No difference in caspase activity was detected between experiment and controls.

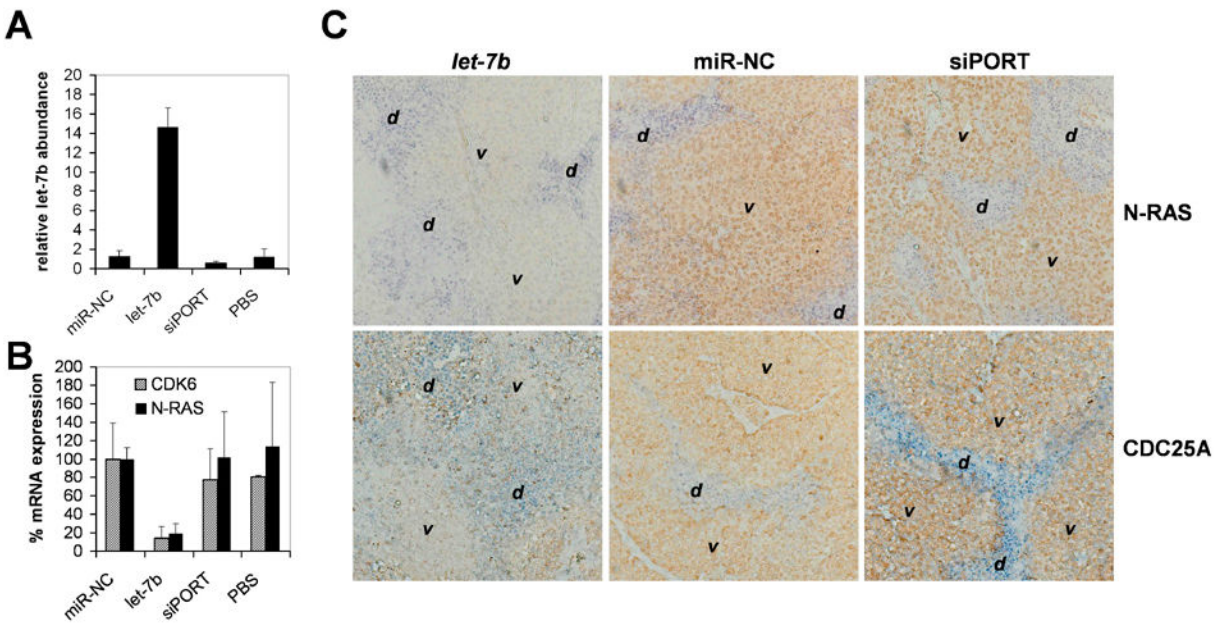

Figure 3. *let-7* accumulation and activity in H460 tumor xenografts

(A) Relative *let-7b* abundance in H460 tumors. qRT-PCR was performed using primers specific for *let-7b* and total RNA from tumors harvested 1 day post the final treatment. Ct values were used to calculate absolute *let-7b* copy numbers and expressed relative to the average expression in control tumors (1.0). Averages and standard deviations of 3 animals (miR-NC and *let-7b*) or 2 animals (siPORT, PBS) are shown. **(B)** qRT-PCR analysis measuring mRNA levels of *let-7* targets. qRT-PCR was carried out using total RNA from H460 tumors harvested on day 21 and primers specific for the CDK6 and N-RAS transcripts. Raw Ct values were normalized to the ones of GAPDH, a house-keeping gene not regulated by *let-7b*, and graphed relative to CDK6 and N-RAS expression in miR-NC treated tumors (100%). Averages and standard deviations of 3 animals (miR-NC and *let-7b*) or 2 animals (siPORT, PBS) are shown. **(C)** Immunohistochemistries showing protein expression of the *let-7* targets N-RAS and CDC25A. Staining of tumors treated with *let-7b* or of control tumors were carried out in parallel. *v*, area containing viable H460 tumor cells; *d*, area containing dead cells, cell debris or cells undergoing cell death.

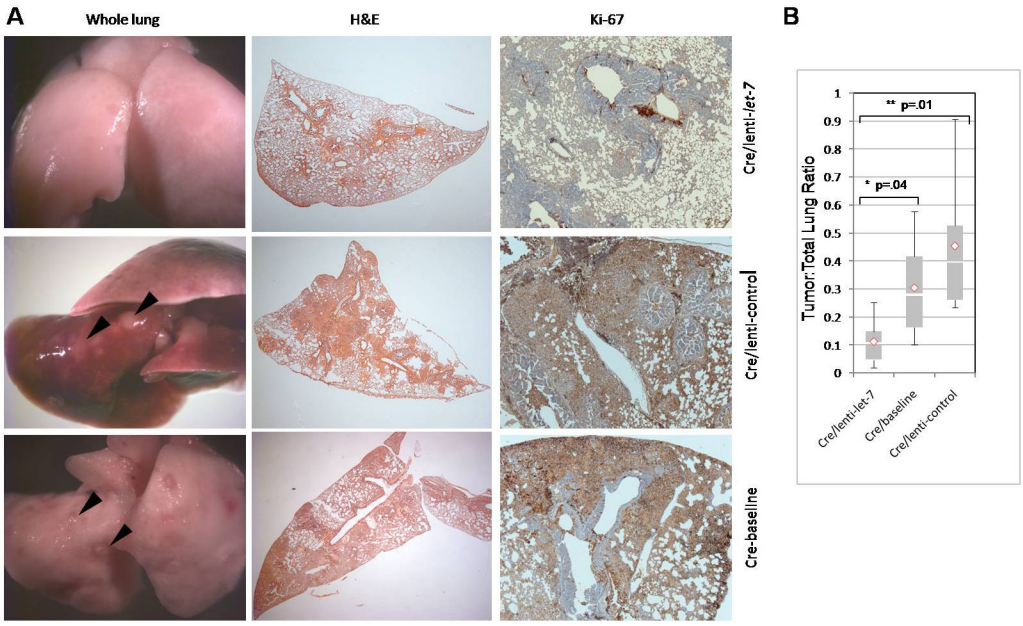

Figure 4. *let-7* reduces lung tumor burden in an autochthonous NSCLC model

Whole lungs, tumor histologies and immunohistochemistries specific for Ki-67 are shown. **(A)** (left and center panels, top) *LSL-K-ras G12D* mice administered with Ad-*Cre* (5×10^8) pfu for 10 weeks then lenti-*let-7* (1×10^6 ifu) for four weeks display reduced lung lesions, hyperplasias and adenomas compared to (left and center panels, center) *LSL-K-ras G12D* mice treated with Ad-*Cre* (5×10^8) for 10 weeks then the empty lenti-control (1×10^6 ifu) for four weeks and (left and center panels, bottom) baseline animals, which were sacrificed at 10 weeks after Ad-*Cre* infection. (Right panel) Ki-67 staining of lungs. **(B)** Quantitative analysis of tumor burden in LSL-*K-ras* G12D animals treated with Ad-*Cre* and lenti-*let-7* (n=6) versus *LSL-K-ras G12D* animals treated with Ad-*Cre* and lenti-control (n=6) and Ad-*Cre* treated baseline animals (n=6). The ratios of tumor area versus normal lung area are presented as a box-and-whisker plot. Boxes represent interquartile ranges (between the 25th and 75th quartiles) and the two-tailed p-value is indicated. The total range, mean (◇), and median (blank bar) are shown. pfu, plaque forming units; ifu, infectious units.